# Virtual Photon Approximation for Three-Body Interatomic Coulombic Decay

Robert Bennett,[1,2] Petra Votavová,[3] Přemysl Kolorenč,[3] Tsveta Miteva,[4] Nicolas Sisourat,[4] and Stefan Yoshi Buhmann[1,2]
[1]*Physikalisches Institut, Albert-Ludwigs-Universität Freiburg, Hermann-Herder-Str. 3, 79104 Freiburg, Germany*
[2]*Freiburg Institute for Advanced Studies (FRIAS) Albertstr. 19, 79104 Freiburg, Germany*
[3]*Charles University, Faculty of Mathematics and Physics, Institute of Theoretical Physics, V Holešovičkách 2, 180 00 Prague, Czech Republic*
[4]*Sorbonne Université, CNRS, Laboratoire de Chimie Physique—Matière et Rayonnement, F-75005 Paris, France*

(Received 25 November 2018; revised manuscript received 28 January 2019; published 15 April 2019)

Interatomic Coulombic decay (ICD) is a mechanism that allows microscopic objects to rapidly exchange energy. When the two objects are distant, the energy transfer between the donor and acceptor species takes place via the exchange of a virtual photon. On the contrary, recent *ab initio* calculations have revealed that the presence of a third passive species can significantly enhance the ICD rate at short distances due to the effects of electronic wave function overlap and charge transfer states [Phys. Rev. Lett. **119**, 083403 (2017)]. Here, we develop a virtual photon description of three-body ICD, allowing us to investigate retardation and geometrical effects which are out of reach for current *ab initio* techniques. We show that a passive atom can have a significant influence on the rate of the ICD process at fairly large interatomic distances, due to the scattering of virtual photons off the mediator. Moreover, we demonstrate that in the retarded regime ICD can be substantially enhanced or suppressed depending on the position of the ICD-inactive object, even if the latter is far from both donor and acceptor species.

DOI: 10.1103/PhysRevLett.122.153401

Interatomic Coulombic decay (ICD) is an ultrafast process by which energy can be transferred between microscopic objects (e.g., atoms, ions, clusters, quantum dots). First predicted just over two decades ago [1], it involves an excited donor species that then decays and transmits sufficient energy to a neighboring acceptor species that the latter can be ionized. Since most of the excess energy of the donor is spent ejecting an electron from the acceptor, a slow electron is left in the continuum [2]. As well as being one of the experimental signatures of ICD [3], it has been shown that such slow electrons can be damaging in a biological context [4].

The ICD rate is an important property in characterization of the process. However, its computation is a challenging task. Most calculations of ICD rates use techniques adapted from computational quantum chemistry, necessitated by the donor and acceptor species being very closely spaced so that orbital overlap has a dramatic effect on the system [5,6]. However, at slightly larger distances it is possible to use a "virtual photon approximation" [5]. There, the donor and acceptor are considered as separate objects coupled via the quantized electromagnetic field. This results in a simple analytic expression for the rate that depends on the single-body decay rate of the donor, the photoionization cross section of the acceptor and their mutual separation. This expression is often used as a consistency check for the large-distance behavior of a particular quantum chemical calculation. Furthermore, an analytical formula for the ICD rate provides a simple means to investigate large systems based on the decomposition of the clusters into pairs [7,8].

Recently, a type of three-body ICD mechanism known as superexchange ICD was proposed [9]. Based on extensive *ab initio* calculations, it was shown that the rate of energy transfer can be substantially enhanced in the presence of a third ICD-inactive mediating atom. A related process has also been demonstrated numerically in electronic decay through $OC_nF_2$ chains [10]. However, there is no equivalent of the virtual photon approximation for the three-body ICD process. This problem can be solved by making use of a macroscopic quantum electrodynamics (QED) based approach recently put forward in Ref. [11] where the effects of the environment near the decaying pair can be accounted for. It should be mentioned that the corresponding situation for Förster resonant energy transfer (FRET) has been investigated previously [12,13].

In this Letter we develop the virtual photon approximation for three-body ICD and find agreement with *ab initio* data in the relevant regimes. The new theory allows us to readily investigate retardation and geometrical effects in three-body ICD, providing insight into long-range energy transfer processes that are out of reach for current *ab initio* techniques. Our method is based on the recently derived formula for the ICD rate in a generic medium [11]:

$$\Gamma = 2\pi^2 \sum_{\text{channels}} \gamma_{\mathrm{D}} \sigma_{\mathrm{A}}(\hbar\omega_{\mathrm{D}}) \mathrm{Tr}[\mathbb{G}(\mathbf{r}_{\mathrm{A}}, \mathbf{r}_{\mathrm{D}}, \omega_{\mathrm{D}}) \cdot \mathbb{G}^*(\mathbf{r}_{\mathrm{D}}, \mathbf{r}_{\mathrm{A}}, \omega_{\mathrm{D}})], \tag{1}$$

 

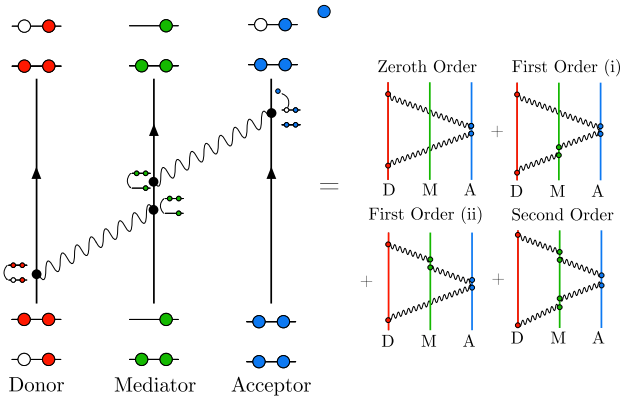


FIG. 1. The process we consider. An excited donor relaxes to its ground state, emitting a photon which eventually ionizes an acceptor. On the way, this photon may interact with a mediating atom, whose contribution is considered perturbatively as far as is consistent with the perturbation theory that leads to Eq. (1).

where $\gamma_{\mathrm{D}}$ is the free-space decay rate of the donor species and $\sigma_{\mathrm{A}}(\hbar\omega_{\mathrm{D}})$ is the photoionization cross section of the acceptor. The quantity $\mathbb{G}(\mathbf{r},\mathbf{r}',\omega)$ is the Green's tensor of the Helmholtz equation, describing propagation of excitations of frequency $\omega$ from point $\mathbf{r}'$ to $\mathbf{r}$, taking into account the effects of any environment that may exist between or around the donor and acceptor.

We consider a process where an ICD-inactive atom absorbs the virtual photon emitted from the donor and then re-emits this photon, which is subsequently absorbed by the acceptor, ejecting an electron and finishing the ICD process, as illustrated in Fig. 1.

In order to calculate the rate in this situation, we need an explicit form of the Green's tensor for an environment consisting of a single atom. To obtain this we expand the Green's tensor in a Born series around a known "background" Green's tensor $\mathbb{G}^{(0)}$ [14], which could represent a vacuum, a homogeneous medium, a dielectric plate, or any other geometry for which the Green's tensor is analytically known. We have the following:

$$\mathbb{G}(\mathbf{r},\mathbf{r}',\omega)=\mathbb{G}^{(0)}(\mathbf{r},\mathbf{r}',\omega)+\mu_0\omega^2\int d^3\mathbf{s}\,n(\mathbf{s})\mathbb{G}^{(0)}(\mathbf{r},\mathbf{s},\omega)\cdot\boldsymbol{\alpha}(\omega)\cdot\mathbb{G}(\mathbf{s},\mathbf{r}',\omega) \tag{2}$$

where $\boldsymbol{\alpha}(\omega)$ is the polarizability tensor of the mediating atom at frequency $\omega$, and $\mu_0$ is the vacuum permeability. The integral runs over the volume of any dielectric bodies not included in $\mathbb{G}^{(0)}$, each of which has a position-dependent atomic number density $n(\mathbf{r})$. Equation (2) is exact but infinitely recursive, nevertheless a result for any order can be found by repeated substitution. For example the first order approximation can be obtained by substituting $\mathbb{G}\to\mathbb{G}^{(0)}$ on the right-hand side of Eq. (2). The result is the Green's tensor for the background environment described by $\mathbb{G}^{(0)}$, with a single atom added. The terms in this approximation can be visualized as scattering from $\mathbf{r}'$ to $\mathbf{r}$ via intermediate scattering points $\mathbf{s}$ with coupling strength determined by $\boldsymbol{\alpha}(\omega)$. In our system the mediator is a single atom in a vacuum at position $\mathbf{r}_{\mathrm{M}}$, which we describe via a Dirac delta function number density $n(\mathbf{s})=\delta(\mathbf{s}-\mathbf{r}_{\mathrm{M}})$. Using this in the first-order approximation to the Born series [Eq. (2)] we have

$$\mathbb{G}^{(1)}(\mathbf{r},\mathbf{r}',\omega)=\mathbb{G}^{(0)}(\mathbf{r},\mathbf{r}',\omega)+\mu_0\omega^2\mathbb{G}^{(0)}(\mathbf{r},\mathbf{r}_{\mathrm{M}},\omega)\cdot\boldsymbol{\alpha}(\omega)\cdot\mathbb{G}^{(0)}(\mathbf{r}_{\mathrm{M}},\mathbf{r}',\omega) \tag{3}$$

The higher-order terms depend on self-interactions, corresponding to quantities like $\mathbb{G}^{(0)}(\mathbf{r}_{\mathrm{M}},\mathbf{r}_{\mathrm{M}},\omega)$. These are already taken into account by using an observed polarizability that includes QED corrections [15], meaning that Eq. (3) is in principle an exact relation. Crucially, $\mathbb{G}^{(1)}$ now only depends on the vacuum Green's tensor $\mathbb{G}^{(0)}$ and the polarizability $\boldsymbol{\alpha}$, which are both well known (see, e.g., Ref. [16] and the Supplemental Material [17]). Substituting the Green's tensor [Eq. (3)] into the rate formula [Eq. (1)], one finds three types of term which are of zeroth, first, and second order in the polarizability. One can then proceed to use the vacuum Green's tensor in these four terms and work out ICD rates for arbitrary arrangements of donor, mediator, and acceptor. However, the resulting expressions are extremely complex and lengthy (see Supplemental Material [17]), so they do not provide much insight or intuition. We can considerably simplify calculations by anticipating that the transition wavelength of the donor we consider is far longer than the few Ångströms at which ICD processes are active. This means we are in the nonretarded (static) regime, in which the Green's tensor is given by (see, e.g., Ref. [16])

$$\mathbb{G}^{(0)}_{\mathrm{NR}}(\mathbf{r},\mathbf{r}',\omega)=-\frac{c^2}{4\pi\omega^2\rho^3}(\mathbb{I}-3\mathbf{e}_\rho\otimes\mathbf{e}_\rho) \tag{4}$$

where $\rho=|\mathbf{r}-\mathbf{r}'|$, $\mathbf{e}_\rho$ is a unit vector in the direction of $\mathbf{r}-\mathbf{r}'$ and $\mathbb{I}$ is the $3\times3$ identity matrix. We also simplify the derivation by assuming that the mediator has a real, isotropic, and frequency-independent polarizability $\boldsymbol{\alpha}(\omega)=\alpha\mathbb{I}$. It is also useful to work with the polarizability volume $\alpha/(4\pi\varepsilon_0)$ (where $\varepsilon_0$ is the vacuum permittivity) rather than the polarizability itself so for the rest of this article we make the replacement $\alpha/(4\pi\varepsilon_0)\mapsto\alpha$. Substituting the nonretarded Green's tensor [Eq. (3)] into the rate formula [Eq. (1)], we find

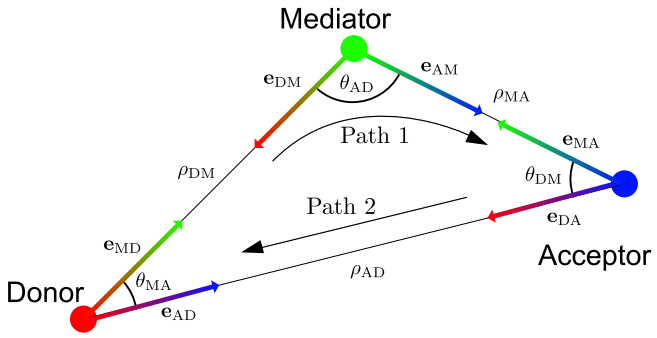


FIG. 2. Definitions of geometrical quantities. Path 1 and Path 2 indicate the forward and backward parts of the closed trajectory corresponding to the first order diagram (i) (cf. Fig. 1).

$$\Gamma_{NR} = C_6\left(\frac{1}{\rho_{AD}^6} + \frac{3\alpha^2}{2\rho_{MD}^6\rho_{MA}^6}(1+\cos^2\theta_{AD}) - \frac{\alpha}{\rho_{AD}^3\rho_{DM}^3\rho_{MA}^3}(1+3\cos\theta_{DM}\cos\theta_{MA}\cos\theta_{AD})\right), \tag{5}$$

where we have defined a Hamaker-type coefficient $C_6 = \gamma_D\sigma_A(\hbar\omega_D)(3c^4/4\omega_D^4)$ and written the result in terms of the angles and distances defined in Fig. 2. It is interesting to note that there are certain choices of geometry for which the rate can be slightly lower than in free space [18], but the retardation effects discussed later are much more dramatic so we postpone discussion of suppression until then.

An important special case can be extracted from the general nonretarded rate [Eq. (5)]. This is the rate $\Gamma_{NR}^L$ for a colinear arrangement, in which $\theta_{MA} = \theta_{DM} = 0$ and $\theta_{AD} = \pi$. Then

$$\Gamma_{NR}^L = \frac{C_6}{\rho_{AD}^6}\left(1+\frac{2}{3}u_{NR}+u_{NR}^2\right), \tag{6}$$

where $u_{NR} = \alpha\rho_{AD}^3/(\rho_{DM}^3\rho_{MA}^3)$ is a dimensionless number indicating the strength of the interaction with the mediator, which must be less than unity for our perturbative approach to be applicable. For comparison with recent *ab initio* work [9], we further assume that the mediator is halfway between the donor and acceptor ($\rho_{DM} = \rho_{MA} = \rho_{AD}/2$), giving a very simple result:

$$\Gamma_{NR}^{mid} = C_6\left(\frac{1}{\rho_{AD}^6} + \frac{128\alpha}{\rho_{AD}^9} + \frac{12\,288\alpha^2}{\rho_{AD}^{12}}\right). \tag{7}$$

Equation (7) can now be compared to *ab initio* calculations. As in Ref. [9], we consider the case where the donor and acceptor are both neon, and the mediator is helium. Before making this comparison, however, we note that in Ref. [9] excited configurations of the type $Ne^+He^*Ne$ were excluded from the calculations, meaning we should consider only the static polarizability of the helium, given by $\alpha_{He} = 0.205$ Å$^3$ [19].

We also need a value for the two-body coefficient $C_6$, which can in principle be calculated from known values of the free-space decay rate of the donor $\gamma_D$, the photoionization cross section of the acceptor $\sigma_A(\hbar\omega_D)$ and the transition frequencies involved in the process $\omega_D$. Indeed this can be done for the system of interest here with results coinciding up to small numerical factors, but due to complications of the type discussed in [5], we determine the $C_6$ from *ab initio* calculations. We do this by removing the mediator from the system, and place the neon atoms far enough apart that a $1/\rho_{AD}^6$ distance dependence is seen.

Shown in Fig. 3 is the comparison between the ICD widths given in our new approach by Eq. (7), and the calculated with the *ab initio* Fano-algebraic diagrammatic construction (ADC)-Stieltjes method [6,20] (see Ref. [9] for details of the calculations). As seen in the upper panel, the results deviate significantly from the *ab initio* data if

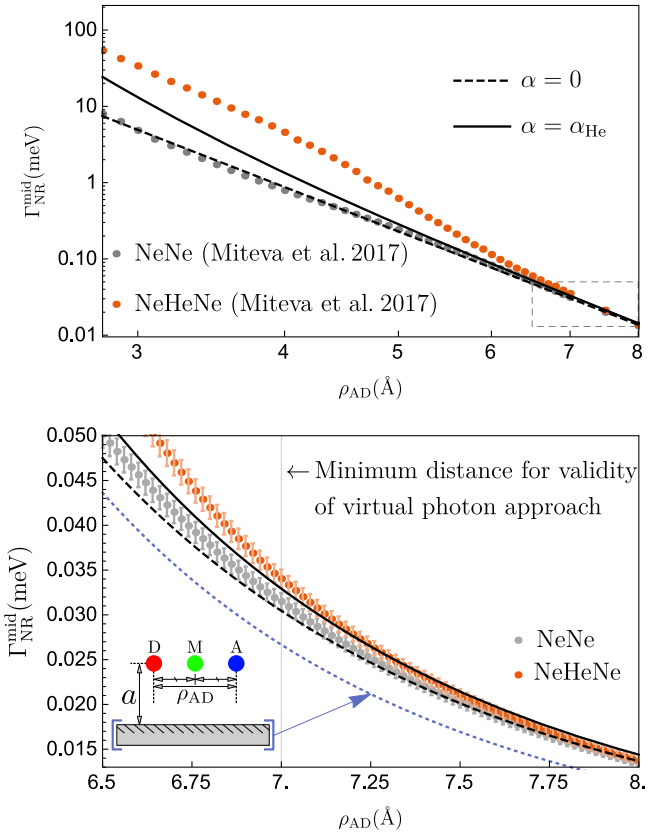


FIG. 3. ICD rate vs donor-acceptor distance, with the mediator placed at the midpoint, $C_6 = 3.6$ eV and $\alpha = \alpha_{He} = 0.205$ Å$^3$. NeNe denotes the situation when the mediator is removed entirely, NeHeNe in the upper plot represents the same data as presented in Ref. [9], while the lower plot contains new high-resolution data calculated for this Letter. The error bars on the *ab initio* data are 3%, which comes from the standard deviation of the decay widths calculated by Fano-ADC-Stieltjes method. In the lower panel we have also included the rate if the NeHeNe trimer is placed $a = 3$ Å away from a perfectly reflecting surface.

$\rho_{AD} \lesssim 7$ Å. This is to be expected for at least two reasons. First, the virtual photon method should fail when there is significant wave function overlap, as discussed in detail in Ref. [5]. Second, the superexchange enhancement seen below 7 Å in Ref. [9] relies on intermediate states that include charge transfer, where the helium gains an electron to become $He^-$, which are not included in our virtual photon approach. The contribution of these charge transfer intermediate states to three-body ICD decreases exponentially with the neon-neon distance; we therefore concentrate on distances larger than 7 Å. As shown in the lower panel of Fig. 3, the ICD widths obtained with both approaches agree well, supporting the general approach taken here.

It should be mentioned that, even without the inclusion of the charge transfer intermediate states, a clear enhancement of the ICD rates is seen. In our approach, any mediator dependence of the rate is to be understood as coming from the mediator's modification of the electromagnetic field that couples the donor and acceptor species, rather than modification of atomic properties themselves.

Finally, we emphasize the general applicability of our approach with an additional example using an inhomogenous macroscopic background, namely a perfectly reflecting plate. Substituting the nonretarded limit of the relevant Green's tensor (see Supplemental Material [17] and Ref. [21]) into Eq. (1), one finds the rate suppression shown in the lower panel of Fig. 3, which is consistent with our earlier two-body work [11].

All the results shown so far are in the nonretarded regime, as can be seen by noting that photon frequencies in Ref. [9] are determined by the $2s^{-1} \rightarrow 2p^{-1}$ transition of $Ne^+$, which has a wavelength of 460 Å. Retardation sets in at the transition wavelength divided by $2\pi$, which for this system is an order of magnitude longer than all considered separations of donor, mediator, and acceptor. Nevertheless, since the method used here intrinsically includes retardation [11], we can put the three-body ICD process into a broader context by considering the consequences of using a donor with a higher transition frequency, or, equivalently, large spacing between the three atoms. Physical systems which may fulfill these criteria include highly charged or hollow ions, as discussed in detail in our previous work [11], and experimentally observed in the context of Förster resonance energy transfer in solids [22]. One of the most striking consequences of retardation is that the ICD rate can oscillate in space if the mediator is placed anywhere other than on the line joining donor and acceptor. To see this, we use the Green's tensor in its retarded (far-field) limit as found in, e.g., Ref. [16] and the Supplemental Material [17],

$$\mathbb{G}_R^{(0)}(\mathbf{r}, \mathbf{r}', \omega) = \frac{e^{i\omega\rho/c}}{4\pi\rho}(\mathbb{I} - \mathbf{e}_\rho \otimes \mathbf{e}_\rho), \tag{8}$$

in Eq. (1) via Eq. (3), giving a rate $\Gamma_R$. For a general mediator position, this is a very long and unwieldy expression, so we only report an explicit formula for the rate $\Gamma_R^L$ in the colinear arrangement

$$\Gamma_R^L = \frac{C_2}{\rho_{AD}^2}\left[1 + u_R^2 + 2u_R \begin{cases} \cos(2\omega_D \rho_{AM}/c) & \text{if } \theta_{AD} = 0 \\ 1 & \text{if } \theta_{AD} = \pi \end{cases}\right], \tag{9}$$

where $u_R = \alpha\rho_{AD}^2 {\omega_D}^2/(\rho_{AD}\rho_{AM}\rho_{DM}c^2)$ is a dimensionless number describing the strength of the interaction, $\theta_{AD}$ is defined in Fig. 2, and $C_2 = \gamma_D \sigma_A(\hbar\omega_D)/4$. When the mediator is outside the region between donor and acceptor, spatial oscillations occur. This is shown in Fig. 4, where we have plotted the rate [Eq. (9)] for fixed donor and acceptor positions, and a mediator whose position is allowed to vary. It is remarkable that, in the retarded (far-field) regime, the ICD rate between donor and acceptor can be strongly suppressed by placing an ICD-inactive atom *outside* the region between them. Such suppression comes from processes where the mediator interacts once with the electromagnetic field [i.e., the oscillatory term in Eq. (9) is linear in $\alpha$]. This, coupled with the fact that no oscillations occur if $\theta_{AD} = \pi$, demonstrates that the oscillations have their origin in the phase accumulated along the example trajectory indicated in Fig. 2, which is determined by the phase difference between the (mediated) forward path 1 and the (direct) backward path 2.

We briefly mention here that the results presented in Fig. 4 can, in principle, be measured in a small cluster composed of two heavy rare gas atoms and one (or few) helium atom(s). Taking two heavy atoms allows us to reach the retarded regime after the core ionization of one of these atoms. Furthermore, helium is so light and inert that the helium atom can be found nearly anywhere around other rare gas atoms (see, e.g., Refs. [23,24]). Using a pump probe setup as in Ref. [25] and a coincidence ion-momenta spectrometer (see, e.g., Refs. [26,27]), it would be possible to measure the decay rates as functions of the helium position relative to the heavy atom pair.

Our theory can be extended to the many-mediator case using a simple approach where either a sum over a set of weakly interacting mediators is taken, or they are considered as a macroscopic background medium in the two-body case. A full calculation is not straightforward since both the general formula [Eq. (1)] and the Green's tensor [Eq. (3)] are perturbative in the polarizability of the atoms. A more advanced approach is also possible, where one mediator (e.g., the decaying pair's nearest neighbor) is considered microscopically, while the rest of the cluster is taken into account as a macroscopic background like the reflecting surface shown in Fig. 3. The latter has the advantage that an analytically known Green's tensor is nonperturbative in $\alpha$, already taking into account the

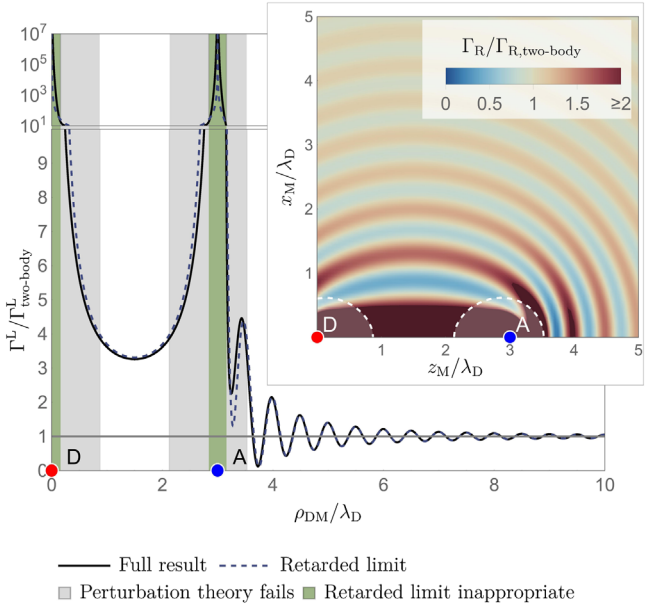


FIG. 4. (Main plot) Three-body far-field ICD rate $\Gamma^L_R$ given by Eq. (9) (dashed lines), normalized to the two-body rate given by setting $\alpha$ to zero in that equation. The donor is at the origin, the acceptor is placed three wavelengths $\lambda_D$ away ($\rho_{AD} = 3\lambda_D$), and the polarizability volume is $(\lambda_D/4)^3$. Also shown as a solid line is the full result at any distance (neither retarded nor nonretarded), showing that the retarded limit [Eq. (9)] is valid further than $\lambda_D/(2\pi)$ from donor or acceptor. However, the perturbative approach used here becomes unreliable if $u_R > 1$, which turns out to be a more stringent condition than the retarded limit, as shown. The inset shows a plot of the generalization of Eq. (9) to two dimensions using the same parameters and placing the acceptor on the $z$ axis. There the regions bounded by white dashed lines represent the region where our perturbation theory becomes unreliable.

microscopic interactions between the atoms making up the environment to all orders in their polarizability. This would circumvent the delicate perturbation theory mentioned above, while still describing one mediator microscopically. Finally, the dynamical polarizability could even be used in Eq. (3) in order to account for possible resonances between the virtual photon energy and the excited states of the mediator.

In this Letter we have presented a virtual photon approximation for three-body ICD by taking advantage of the recently introduced theoretical approach for calculation of the rate in arbitrary environments [11]. Our approach is consistent with earlier *ab initio* work, and goes beyond it by exploring the retarded regime and including external macroscopic environments. In the context of the former we make a surprising prediction that a carefully placed mediator can cause almost complete suppression of the rate in an experimentally accessible situation, providing a powerful tool for the control and manipulation of ICD rates.

R. B. and S. Y. B. thank Akbar Salam for fruitful discussions. R. B. acknowledges financial support by the Alexander von Humboldt Foundation and S. Y. B. thanks the Deutsche Forschungsgemeinschaft (Grant No. BU 1803/3-1476). R. B. and S. Y. B. both acknowledge support from the Freiburg Institute for Advanced Studies (FRIAS). P. K. and P. V. acknowledge financial support by the Czech Science Foundation (Project GAČR No. 17-10866S). This project has received funding from Agence Nationale de la Recherche through the Program No. ANR-16-CE29-0016-01.

[1] L. S. Cederbaum, J. Zobeley, and F. Tarantelli, Phys. Rev. Lett. **79**, 4778 (1997).
[2] K. Gokhberg, P. Kolorenč, A. I. Kuleff, and L. S. Cederbaum, Nature (London) **505**, 661 (2014).
[3] S. Marburger, O. Kugeler, U. Hergenhahn, and T. Möller, Phys. Rev. Lett. **90**, 203401 (2003).
[4] B. Boudaïffa, P. Cloutier, D. Hunting, M. A. Huels, and L. Sanche, Science **287**, 1658 (2000).
[5] V. Averbukh, I. B. Müller, and L. S. Cederbaum, Phys. Rev. Lett. **93**, 263002 (2004).
[6] V. Averbukh and L. S. Cederbaum, J. Chem. Phys. **123**, 204107 (2005).
[7] E. Fasshauer, M. Förstel, S. Pallmann, M. Pernpointner, and U. Hergenhahn, New J. Phys. **16**, 103026 (2014).
[8] E. Fasshauer, New J. Phys. **18**, 043028 (2016).
[9] T. Miteva, S. Kazandjian, P. Kolorenč, P. Votavová, and N. Sisourat, Phys. Rev. Lett. **119**, 083403 (2017).
[10] A. I. Kuleff, Chem. Phys. **482**, 216 (2017).
[11] J. L. Hemmerich, R. Bennett, and S. Y. Buhmann, Nat. Commun. **9**, 2934 (2018).
[12] G. J. Daniels and D. L. Andrews, J. Chem. Phys. **116**, 6701 (2002).
[13] A. Salam, J. Chem. Phys. **136**, 014509 (2012).
[14] S. Y. Buhmann and D.-G. Welsch, Appl. Phys. B **82**, 189 (2006).
[15] J. W. Schmidt, R. M. Gavioso, E. F. May, and M. R. Moldover, Phys. Rev. Lett. **98**, 254504 (2007).
[16] S. Y. Buhmann, *Dispersion Forces I—Macroscopic Quantum Electrodynamics and Ground-State Casimir, Casimir-Polder and van der Waals Forces*, Springer Tracts in Modern Physics, Vol. 247 (Springer, Berlin, 2012).
[17] See Supplemental Material at http://link.aps.org/supplemental/10.1103/PhysRevLett.122.153401 for a list of the relevant Green's tensors, as well as the general expression which produces Eqs. (5) and (9) as special cases.
[18] For example, this is true for donor, acceptor, and mediator at the corners of an equilateral triangle whose side length is at least $(15\alpha/11)^{1/3}$.
[19] R. D. Rohrmann, Mon. Not. R. Astron. Soc. **473**, 457 (2018).
[20] P. Kolorenč and N. Sisourat, J. Chem. Phys. **143**, 224310 (2015).
[21] R. Palacino, R. Passante, L. Rizzuto, P. Barcellona, and S. Y. Buhmann, J. Phys. B At. Mol. Opt. Phys. **50**, 154001 (2017).

[22] D. Céolin, J.-P. Rueff, A. Zimin, P. Morin, V. Kimberg, S. Polyutov, H. Ågren, and F. Gel'mukhanov, J. Phys. Chem. Lett. **8**, 2730 (2017).
[23] D. Bressanini and G. Morosi, J. Phys. Chem. A **115**, 10880 (2011).
[24] J. Voigtsberger *et al.*, Nat. Commun. **5**, 5765 (2014).
[25] K. Schnorr *et al.*, Phys. Rev. Lett. **111**, 093402 (2013).
[26] R. Dörner, V. Mergel, O. Jagutzki, L. Spielberger, J. Ullrich, R. Moshammer, and H. Schmidt-Böcking, Phys. Rep. **330**, 95 (2000).
[27] J. Ullrich, R. Moshammer, A. Dorn, R. Dörner, L. P. H. Schmidt, and H. Schmidt-Böcking, Rep. Prog. Phys. **66**, 1463 (2003).